Acta Mech
https://doi.org/10.1007/s00707-026-04651-3

ORIGINAL PAPER

Hayrullah Gun Kadioglu · Mustafa Ozgur Yayli

Free vibration characteristics of triple-walled viscoelastic nanotubes using the stress-driven model

Received: 30 September 2025 / Revised: 3 December 2025 / Accepted: 1 February 2026
© The Author(s) 2026

Abstract In this study, a comprehensive analytical model has been developed to investigate the free vibration behavior of triple-walled viscoelastic nanotubes. The model has been constructed by adapting the equations of motion derived based on the stress-driven approach to the triple-walled beam form and incorporating viscoelastic effects using the Kelvin–Voigt model. A Navier-type solution method has been used to solve the problem, and the results obtained from the analyses have been presented in tables and graphs for detailed evaluation. Thus, it has been observed that the system approaches the single-walled beam behavior with the increase in bond forces, that the increase in the scale parameter raises the natural frequencies, and that viscoelastic damping significantly shapes the dynamic response. Furthermore, the interactions between these parameters have been discussed. In conclusion, this study provides an important contribution to understanding the dynamic behavior of multi-walled nanotubes.

1 Introduction

Accurate modeling of the dynamic behavior of nanoscale structures has gained significant importance in recent years with the development of nanotechnology-based engineering applications. Multi-walled carbon nanotubes (MWCNTs), used in nanoelectromechanical systems (NEMS), sensors, biomedical devices, and energy harvesting systems, are among the most noteworthy nanostructures due to their high elastic moduli, low densities, and excellent mechanical strength. Triple-walled nanobeams (TWNs), one such structure, are a special research topic in terms of dynamic analysis due to their complex structures that have been constructed by internal vdW (van der Waals) interactions and multiple boundary conditions. However, existing studies in the literature have mostly been limited to single- or double-walled nanotubes, and the behavior of triple-walled configurations under viscoelastic and nonlocal effects has not been sufficiently addressed.

Classical continuum theories largely lose their validity for structures at the nanoscale, where size effects are significant. In this context, nonlocal elasticity theories that have been developed in recent years provide a more suitable mathematical framework for nanostructures by modeling long-range interactions at the atomic level. However traditional nonlocal theory contains some physical inconsistencies; therefore, they create difficulties in applying boundary conditions and physical interpretation. The stress-driven nonlocal elasticity theory, developed to overcome these limitations, offers a more consistent approach both physically and mathematically.

In this context, some studies in the literature are as follows.

Wang et al. [1] have investigated the free vibration of multi-walled carbon nanotubes using the differential quadrature method, employing the Timoshenko beam theory, a more advanced beam theory that accounts for

H. G. Kadioglu (✉)
Technical Sciences Vocational School, Department of Construction, İstanbul Arel University, Istanbul, Turkey
e-mail: hayrullahgunkadioglu@arel.edu.tr

M. O. Yayli
Faculty of Engineering, Department of Civil Engineering, Bursa Uludag University, Bursa, Turkey

Published online: 20 February 2026

shear effects. Natsuki et al. [2] have studied the vibration characteristics of simply supported double-walled carbon nanotubes (DWCNTs) using Euler–Bernoulli beam theory (EBT) and have indicated that the resonance frequencies differ when the inner and outer nanotubes vibrate in the same or opposite directions in the nonaxial modes arising due to van der Waals interactions. Furthermore, Natsuki et al. [3] have also researched the free vibration of double-walled carbon nanotubes in an elastic medium. Yan et al. [4] have examined the instability behavior of fluid-filled triple-walled carbon nanotubes using the Euler–Bernoulli beam model and the Galerkin discretization method, revealing the significant role of van der Waals interactions on natural frequencies and critical flow velocities. Zhang et al. [5] have investigated the free vibration of double-walled carbon viscoelastic nanotubes embedded in a viscoelastic medium using nonlocal elasticity theory and the transfer function method. Pentaras and Elishakoff [6] have probed the dynamic behavior of triple-walled carbon nanotubes using the Petrov–Galerkin method. Artan and Tepe [7] have examined the mechanical behavior of single-walled curved carbon nanotubes loaded in a direction perpendicular to the plane based on nonlocal elasticity theory using the initial value method. This work has been extended and developed by Tepe [8] for double-walled carbon nanotubes.

Aydogdu [9] have addressed the axial vibration response of DWCNTs through both local and nonlocal rod models, while explicitly incorporating the influence of van der Waals forces. Building on similar modeling approaches, Ehyaei and Daman [10] have investigated imperfect DWCNTs embedded in an elastic foundation using nonlocal Timoshenko beam theory, where natural frequencies were obtained through the Navier method. Likewise, Murmu et al. [11] have explored magnetically sensitive DWCNTs exposed to a longitudinal magnetic field by developing an equivalent nonlocal double-beam model that accounts for Lorentz forces derived from Maxwell's relation.

In another contribution, Shen et al. [12] have analyzed the vibrational characteristics of DWCNT-based nanomechanical sensors subjected to initial axial stress by employing nonlocal Euler–Bernoulli beam theory (EBT) combined with the transfer function technique. Dihaj et al. [13] have considered the transverse oscillations of chiral DWCNTs embedded in an elastic matrix, adopting Eringen's nonlocal elasticity along with EBT. Similarly, Rakrak et al. [14] have extended this line of research by focusing on the free vibration behavior of chiral DWCNTs within the same theoretical framework.

Kiani [15] has examined elastically supported DWCNTs subjected to axially varying magnetic fields through the application of nonlocal Rayleigh beam theory. In subsequent works, Kiani [16] has broadened the investigation by including Rayleigh, Timoshenko, and higher-order nonlocal models to describe the free vibration of DWCNTs under longitudinally varying magnetic fields. Moreover, Lee and Chang [17] have derived an analytical solution for the coupled vibration of fluid-conveying DWCNTs in the context of nonlocal elastic theory, while Aydogdu and Arda [18] have concentrated on the torsional vibration response of DWCNTs using the same theoretical approach. Mohammadi et al. [19] numerically investigated the nonlinear vibrations of triple-walled carbon nanotubes carrying viscous fluids based on the Pasternak foundation. Channakote et al. [20] investigated the transport dynamics of carbon nanotube-based nanofluids under the influence of electroosmotic ciliary motion in biological environments using a microcapillary flow model. Zeighampour and Beni [21] investigated the vibration and instability behavior of double-walled carbon nanotubes carrying fluid using a modified couple stress theory and a visco-Pasternak fundamental model. Yıldız and Esen [22] modeled the thermo-mechanical buckling behavior of nanosmart sandwich plates, considering Casimir, van der Waals, and electrostatic forces. Özmen and Esen [23] investigated the effect of Casimir, van der Waals, and electrostatic forces on the vibration and buckling behavior of nanoswitches.

Romano and Barretta [24] have proposed a new stress-based approach to investigate small-scale effects in nanobeams. Furthermore, Romano and Barretta [25] have highlighted the differences between their developed stress-based elasticity theory and Eringen's nonlocal elasticity theory, as well as the advantages offered by this new approach. Luciano et al. [26] have carried out the free vibration analysis of nanobeams based on the stress-driven nonlocal theory for elastic boundary conditions. Oskouie et al. [27] have investigated the free vibration behavior of nanobeams using Timoshenko beam theory and stress-driven nonlocal and strain gradient approaches. Akpınar et al. [28] have carried out the dynamic behavior of viscoelastic functional graded and short fiber-reinforced nanobeams, including inertial effects, using the stress-driven model with the help of Fourier series and Stokes transformations. Altekin et al. [29] have examined the bending behavior of ring-shaped nanoplatens under axial symmetric loading within the framework of classical plate theory and stress-based nonlocal theory, revealing the significant effects of small-scale effects and geometric parameters on stiffness using numerical methods. Atacan and Yükseler [30] have investigated the nonlinear sudden buckling instability of functionally graded shallow nanoarches within the framework of stress-based nonlocal elasticity theory, demonstrating that parameters such as support stiffness, power-law exponent, modular

ratio, and thinness, creating different effects in local and nonlocal regimes, and that these interactions play a critical role in nanostructure design. Beni [31] investigated the free vibration and static torsion behavior of electromechanically coupled flexoelectric micro/nanotubes using a gradient-based continuity theory. Beni [32] has, for the first time, analytically investigated the torsion behavior of porous flexoelectric microtubes made from functionally graded materials using a modified nonlinear flexoelectric theory.

Many studies using different theories to model other nanoscale effects can be added to these studies [33–51].

Viscoelasticity is a critical property that reflects the time-dependent mechanical behavior of nanomaterials [52]. Due to the fact that material deformation contains both elastic and time-dependent (viscous) components, viscoelastic effects cannot be ignored in dynamic analyses [53]. In this context, considering viscoelastic material models in the vibration analysis of nanobeams is critical for reflecting the dynamic characteristics of the system more realistically.

Although there are numerous studies in the current literature on the vibration and mechanical behavior of nanotubes, comprehensive analytical models considering the free vibration characteristics of multi-walled viscoelastic nanotubes remain limited. In particular, the simultaneous investigation of bond forces, scale effects, and viscoelastic damping mechanisms has not been sufficiently addressed in the literature. In this study, an analytical model based on a stress-driven approach has been developed and solved using the Navier-type solution method to investigate the free vibration behavior of triple-walled viscoelastic nanotubes. In this context, the main reason for choosing the stress-driven model in this study is that it can eliminate the paradoxical situation that arises in nonlocal elastic theory. Finally, the results obtained reveal the effects of bond forces, scale parameter, and viscoelastic effects on the dynamic response of the system, and the study provides important contributions to understanding the dynamic behavior of multi-walled nanotubes.

2 Defining theoretical formulas

In this section, the governing equations are derived based on the stress-driven nonlocal elasticity theory. The formulation begins by establishing the relation between the bending curvature $\left(W_{x,t}\right)$ and the transverse displacement (φ) at time (t) [24]:

$$W(x,t) = \varphi^{(2)}(x) \tag{1}$$

Within the stress-driven model, the convolution principle with an integral kernel is adopted [24]:

$$W(x,t) = \int_0^L \chi(x-\xi)C(\xi)M(\xi,t)d\xi \tag{2}$$

Here, ξ denotes the position vector, and t represents time. The local elastic compliance C is expressed as [24]:

$$C = \frac{1}{EI} \tag{3}$$

The kernel function χ is defined in the following form [24]:

$$\chi(x) = \frac{1}{2L_C}\exp\left(-\frac{|x|}{L_C}\right) \tag{4}$$

In this expression, L_C refers to the characteristic length of the nanobeam, defined as $(L_C = \lambda L)$. The dimensionless nonlocal parameter (λ) introduces size-dependent effects into the formulation. This parameter ensures consistency with nanoscale experimental observations, while the model reduces to the classical local elasticity case when $\lambda = 0$.

The bending moment M is formulated as:

$$M = \int_A \sigma_x y dA \tag{5}$$

where σ_x represents the axial stress. By incorporating the relevant relations, the following differential equation is obtained [26]:

$$W(x,t) - L_C^2 W''(x,t) = M(x,t)C \tag{6}$$

The structural boundary conditions are expressed as [26]:

$$W'(0,t) = \frac{1}{L_C} W(0,t) \tag{7}$$

$$W'(L,t) = \frac{1}{L_C} W(L,t) \tag{8}$$

According to D'Alembert's principle of dynamic equilibrium, the governing condition is given by [26]:

$$M''(x,t) = -m\ddot{\varphi}(x,t) \tag{9}$$

Where m denotes the mass per unit length of the nanobeam and $\ddot{\varphi}(x,\ t)$ is the second derivative of the transverse displacement with respect to time. Finally, by substituting the material parameters and applying Eqs. (1), (6), and (9), the following expression is obtained [26]:

$$EI\varphi^{(4)}(x,t) - EI\gamma\varphi^{(6)}(x,t) = -\rho A\ddot{\varphi}(x,t) \tag{10}$$

Here,γ has been redefined as the scale parameter.

When van der Waals bond forces are included for a triple-walled beam, the equation of motion is obtained as follows.

$$-EI_1\gamma\varphi_1^{(6)} + EI_1\varphi_1^{(4)} = -\rho A_1\ddot{\varphi}_1 + c_1(\varphi_2 - \varphi_1) \tag{11}$$

$$-EI_2\gamma\varphi_2^{(6)} + EI_2\varphi_2^{(4)} = -\rho A_2\ddot{\varphi}_2 + c_2(\varphi_3 - \varphi_2) - c_1(\varphi_2 - \varphi_1) \tag{12}$$

$$-EI_3\gamma\varphi_3^{(6)} + EI_3\varphi_3^{(4)} = -\rho A_3\ddot{\varphi}_3 - c_2(\varphi_3 - \varphi_2) \tag{13}$$

Here, c_1 is the bond force connecting the wall with radius R_1 to the wall with radius R_2 in the triple-walled nanotube shown in Fig. 1. c_2 is the bond force connecting the wall with radius R_2 to the wall with radius R_3. Each wall is considered to have equal thickness, and the analyses have been carried out accordingly. Thus, the area and polar moments of inertia of the cross sections are obtained as follows.

$$I_1 = \int_{R_1-\frac{a}{2}}^{R_1+\frac{a}{2}} \pi r^3 dr \tag{14}$$

$$I_2 = \int_{R_2-\frac{a}{2}}^{R_2+\frac{a}{2}} \pi r^3 dr \tag{15}$$

$$I_3 = \int_{R_3-\frac{a}{2}}^{R_3+\frac{a}{2}} \pi r^3 dr \tag{16}$$

$$I = \int_{R_1-\frac{a}{2}}^{R_3+\frac{a}{2}} \pi r^3 dr \tag{17}$$

$$A_1 = \int_{R_1-\frac{a}{2}}^{R_1+\frac{a}{2}} \pi r dr \tag{18}$$

$$A_2 = \int_{R_2-\frac{a}{2}}^{R_2+\frac{a}{2}} \pi r dr \tag{19}$$

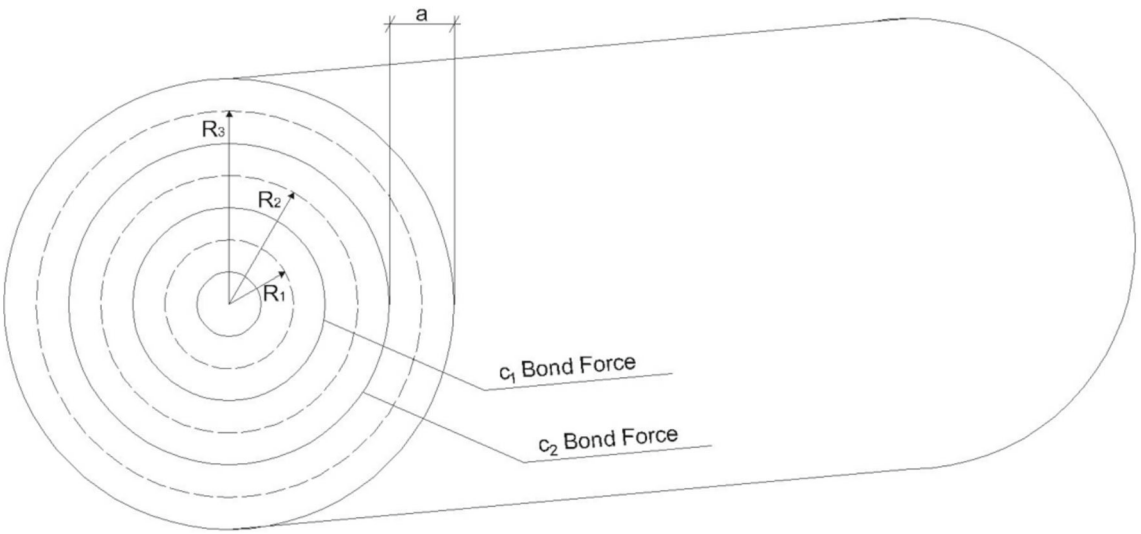


Fig. 1 Cross section of a triple-walled nanotube

$$A_3 = \int_{R_3-\frac{a}{2}}^{R_3+\frac{a}{2}} \pi r dr \tag{20}$$

$$A = \int_{R_1-\frac{a}{2}}^{R_3+\frac{a}{2}} \pi r dr \tag{21}$$

The above equations were obtained for a homogeneous triple-walled beam. If the Kelvin–Voigt viscoelastic model is incorporated into the system to analyze the time-dependent responses of this beam, the equations of motion transform into the following form.

$$\left(1 + t_d \frac{\partial}{\partial t}\right)\left(-EI_1\gamma\varphi_1^{(6)} + EI_1\varphi_1^{(4)}\right) + (\rho A_1\ddot{\varphi}_1 - c_1(\varphi_2 - \varphi_1)) = 0 \tag{22}$$

$$\left(1 + t_d \frac{\partial}{\partial t}\right)\left(-EI_2\gamma\varphi_2^{(6)} + EI_2\varphi_2^{(4)}\right) + (\rho A_2\ddot{\varphi}_2 - c_2(\varphi_3 - \varphi_2) + c_1(\varphi_2 - \varphi_1)) = 0 \tag{23}$$

$$\left(1 + t_d \frac{\partial}{\partial t}\right)\left(-EI_3\gamma\varphi_3^{(6)} + EI_3\varphi_3^{(4)}\right) + (\rho A_3\ddot{\varphi}_3 + c_2(\varphi_3 - \varphi_2)) = 0 \tag{24}$$

Here, t_d is defined as the viscous damping coefficient. By analytically solving the above equations, it is possible to reveal the fundamental parameters that determine the dynamic behavior of triple-walled nanotube cross-sectional beams.

3 Solution methodology

In order to solve the two-variable motion equations obtained in the previous section, the displacement function can be selected as follows so that it is suitable for a beam with two simply supported ends in Fig. 2.

$$\varphi_1(x,t) = Y_1 \sin(\beta x)e^{i\omega t} \tag{25}$$

$$\varphi_2(x,t) = Y_2 \sin(\beta x)e^{i\omega t} \tag{26}$$

$$\varphi_3(x,t) = Y_3 \sin(\beta x)e^{i\omega t} \tag{27}$$

$$\beta = \frac{n\pi}{L} \tag{28}$$

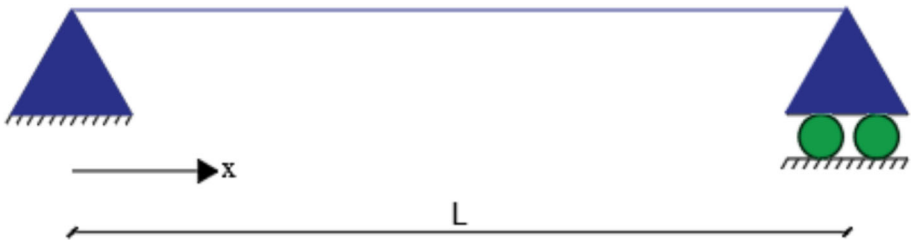


Fig. 2 Boundary condition

Here, n represents the number of modes, L represents the length of the beam, and ω represents the angular frequency. Y_1, Y_2 and Y_3 are unknown coefficients. Substituting the above equations into the equation of motion yields the following mathematical results in matrix form:

$$\begin{bmatrix} \Gamma_{11} & \Gamma_{12} & \Gamma_{13} \\ \Gamma_{21} & \Gamma_{22} & \Gamma_{23} \\ \Gamma_{31} & \Gamma_{32} & \Gamma_{33} \end{bmatrix} \begin{bmatrix} Y_1 \\ Y_2 \\ Y_3 \end{bmatrix} = 0 \tag{29}$$

By setting the determinant of the above 3×3 matrix equal to zero, an equation is obtained from which the angular frequencies of the triple-walled nanotube can be derived. This equation is as follows:

$$\alpha_6\omega^6 + \alpha_5\omega^5 + \alpha_4\omega^4 + \alpha_3\omega^3 + \alpha_2\omega^2 + \alpha_1\omega + \alpha_0 = 0 \tag{30}$$

$$\alpha_6 = -\rho^3 A_1 A_2 A_3 \tag{31}$$

$$\alpha_5 = \mathrm{i}E\beta^4\left(1+\beta^2\gamma\right)\rho^2(A_1A_3I_2 + A_2(A_3I_1 + A_1I_3))t_d \tag{32}$$

$$\begin{aligned}\alpha_4 = \rho(\rho(A_2A_3\left(c_1 + E\beta^4\left(1+\beta^2\gamma\right)I_1\right) + A_1(A_3\left(c_1 + c_2 + E\beta^4\left(1+\beta^2\gamma\right)I_2\right) \\ + A_2\left(c_2 + E\beta^4\left(1+\beta^2\gamma\right)I_3\right))) + E^2\beta^8\left(1+\beta^2\gamma\right)^2(A_3I_1I_2 + (A_2I_1 + A_1I_2)I_3)t_d^2)\end{aligned} \tag{33}$$

$$\begin{aligned}\alpha_3 = \mathrm{i}E\beta^4\left(1+\beta^2\gamma\right)t_d\big(\rho A_3\left(c_1(I_1+I_2) + I_1\left(c_2 + 2E\beta^4\left(1+\beta^2\gamma\right)I_2\right)\right) \\ + \rho A_2\left(c_2I_1 + \left(c_1 + 2E\beta^4\left(1+\beta^2\gamma\right)I_1\right)I_3\right) \\ + \rho A_1\left(c_2I_2 + \left(c_1 + c_2 + 2E\beta^4\left(1+\beta^2\gamma\right)I_2\right)I_3\right) + E^2\beta^8\left(1+\beta^2\gamma\right)^2I_1I_2I_3t_d^2\big)\end{aligned} \tag{34}$$

$$\begin{aligned}\alpha_2 = (\rho A_3(-E\beta^4(1+\beta^2\gamma)I_1(c_2 + E\beta^4(1+\beta^2\gamma)I_2) - c_1(c_2 + E\beta^4(1+\beta^2\gamma)(I_1+I_2))) \\ - \rho A_2(c_1 + E\beta^4(1+\beta^2\gamma)I_1)(c_2 + E\beta^4(1+\beta^2\gamma)I_3) + \rho A_1(-c_2(c_1 + E\beta^4(1+\beta^2\gamma)I_2) \\ - E\beta^4(1+\beta^2\gamma)(c_1 + c_2 + E\beta^4(1+\beta^2\gamma)I_2)I_3) \\ - E^2\beta^8(1+\beta^2\gamma)^2((3E\beta^4(1+\beta^2\gamma)I_1I_2 + c_1(I_1+I_2))I_3 + c_2I_1(I_2+I_3))t_d^2)\end{aligned} \tag{35}$$

$$\begin{aligned}\alpha_1 = iE\beta^4(1+\beta^2\gamma)(E\beta^4(1+\beta^2\gamma)I_1(3E\beta^4(1+\beta^2\gamma)I_2I_3 + 2c_2(I_2+I_3)) + c_1(2E\beta^4(1+\beta^2\gamma)(I_1+I_2)I_3 \\ + c_2(I_1+I_2+I_3)))t_d\end{aligned} \tag{36}$$

$$\begin{aligned}\alpha_0 = E\beta^4(1+\beta^2\gamma)(E\beta^4(1+\beta^2\gamma)I_1(E\beta^4(1+\beta^2\gamma)I_2I_3 + c_2(I_2+I_3)) + c_1(E\beta^4(1+\beta^2\gamma)(I_1+I_2)I_3 \\ + c_2(I_1+I_2+I_3)))\end{aligned} \tag{37}$$

The analytical solution of the equation presented above yields the natural frequency that reveals the dynamic characteristics of a simply supported viscoelastic triple-walled nanotube. Three roots are obtained from the above equation. Which of these roots represents the beam's frequency is discussed in the next section.

The solutions obtained in this study are primarily limited to simple–supported beam boundary conditions. However, approximate solutions can also be obtained for clamped–clamped and clamped–simple–supported cases using the same analysis approach. In this case, the β-value corresponding to the boundary conditions can be taken as $\frac{(2n+1)\pi}{2L}$ and $\frac{(4n+1)\pi}{4L}$, respectively.

Table 1 Changes in dimensionless frequencies of a triple-walled nanotube depending on the scale parameter and bond forces

γ	c_1	c_2	TWNT			SWNT
			Root 1	Root 2	Root 3	λ
0	1	1	8.32233	10.7129	12.0324	9.8696
		5	8.40738	10.8739	15.207	
		10	8.43358	10.8982	18.5606	
	5	1	8.85967	11.8263	14.9194	
		5	9.23871	12.8873	16.7595	
		10	9.36695	13.2522	19.5747	
	10	1	8.94856	11.8612	18.983	
		5	9.38798	13.6631	19.9418	
		10	9.53276	15.03	21.6779	
0.5	1	1	8.50146	10.9257	12.2832	10.1102
		5	8.58223	11.1101	15.3885	
		10	8.60765	11.1387	18.7068	
	5	1	9.05739	12.0901	15.0484	
		5	9.43789	13.0936	16.8972	
		10	9.57073	13.432	19.7035	
	10	1	9.15136	12.1254	19.0803	
		5	9.59696	13.8724	20.0415	
		10	9.74882	15.1988	21.7802	
1	1	1	8.67635	11.1333	12.5302	10.3452
		5	8.75309	11.341	15.5684	
		10	8.77776	11.3742	18.8521	
	5	1	9.25021	12.3482	15.1766	
		5	9.63132	13.2971	17.0344	
		10	9.76837	13.6104	19.8318	
	10	1	9.3493	12.3842	19.1773	
		5	9.80017	14.0792	20.1408	
		10	9.95884	15.3664	21.8822	

4 Result and discussion

In this section, the free vibration frequencies of viscoelastic triple-walled tube-sectioned nanobeams have been obtained, and an attempt has been made to determine which parameters are decisive at these frequencies. First, the following transformations have been carried out to enable comparison of the obtained results with those in the literature.

$$\lambda = \omega L^2 \sqrt{\frac{\rho A}{EI}} \tag{38}$$

$$\tau_d = \frac{t_d}{L^2 \sqrt{\frac{\rho A}{EI}}} \tag{39}$$

Here, λ represents the dimensionless frequency and τ_d is the viscous damping parameter.

The results obtained based on the above parameters are discussed in detail with tables and figures. For this purpose, the material properties $E = 30$ MPa and $\rho = 1$ gr/cm^3 have been selected. The geometric properties have been chosen as$a = 0.5$ nm, $R_1 = 2$ nm, and $L = 10$ nm.

Table 1 presents the variation in frequencies depending on the scale parameter and bond forces. Three distinct roots have been obtained while determining the frequencies of the triple-walled nanotube (TWNT). It is thought that the frequency representing the vibration of the walls in harmony comes from the smallest root, while the other roots represent the vibration modes of the walls that are out of harmony with each other. Thus, when the bond forces are assigned infinitely large values, the smallest root yields the results obtained for a single-walled nanotube (SWNT). The other roots, however, reach frequency values where vibration cannot occur, yielding large values without a common denominator. It can also be stated that the bond forces have a decisive effect on the stiffness of the sections they connect.

Furthermore, Table 1 indicates that dimensionless frequency values increase as the scale parameter increases. The fundamental reason for this is that the scale parameter is related to a stress-based model. Due to this relationship, stress causes more effective transfer within the material's internal structure, thereby increasing rigidity. Consequently, the increase in rigidity also raises the frequency.

Table 2 Change in dimensionless frequencies of a viscoelastic triple-walled nanotube depending on the scale parameter and bond forces

γ	c_1	c_2	TWNT			SWNT
			λ_1	λ_2	λ_3	λ
0	1	1	8.30335 + 0.611805i	10.6835 + 0.934535i	11.9511 + 1.23295i	9.82141 + 0.97409i
		5	8.38916 + 0.602855i	10.8257 + 1.05432i	15.1551 + 1.12211i	
		10	8.4157 + 0.60205i	10.8441 + 1.07481i	18.5215 + 1.10243i	
	5	1	8.83519 + 0.719668i	11.7558 + 1.27825i	14.8925 + 0.781372i	
		5	9.22034 + 0.758377i	12.834 + 1.08526i	16.7199 + 0.935647i	
		10	9.34871 + 0.787714i	13.2013 + 0.968325i	19.5398 + 1.02325i	
	10	1	8.92089 + 0.745035i	11.7893 + 1.28392i	18.9645 + 0.750328i	
		5	9.36375 + 0.807932i	13.6018 + 1.16519i	19.9198 + 0.806162i	
		10	9.50573 + 0.848591i	14.9829 + 1.03165i	21.6516 + 0.899047i	
0.5	1	1	8.48094 + 0.639912i	10.8928 + 0.975526i	12.1967 + 1.301i	10.0584 + 1.02216i
		5	8.56237 + 0.630644i	11.059 + 1.10489i	15.3315 + 1.18091i	
		10	8.58812 + 0.629686i	11.0811 + 1.12822i	18.6638 + 1.15854i	
	5	1	9.03123 + 0.752499i	12.0143 + 1.34186i	15.0187 + 0.822078i	
		5	9.41852 + 0.788897i	13.0365 + 1.14178i	16.8534 + 0.985763i	
		10	9.55191 + 0.81861i	13.3765 + 1.02201i	19.665 + 1.07582i	
	10	1	9.12165 + 0.779931i	12.048 + 1.3482i	19.0601 + 0.78831i	
		5	9.57136 + 0.842179i	13.8059 + 1.2269i	20.0172 + 0.847362i	
		10	9.72053 + 0.884809i	15.1473 + 1.08647i	21.7511 + 0.945165i	
1	1	1	8.65426 + 0.668026i	11.097 + 1.01689i	12.4385 + 1.36868i	10.2897 + 1.07023i
		5	8.73155 + 0.658514i	11.2871 + 1.15508i	15.5062 + 1.24i	
		10	8.75654 + 0.657419i	11.313 + 1.18137i	18.8051 + 1.2148i	
	5	1	9.22235 + 0.785207i	12.2672 + 1.40539i	15.144 + 0.862998i	
		5	9.61088 + 0.819148i	13.2363 + 1.19816i	16.986 + 1.03629i	
		10	9.74895 + 0.849034i	13.5503 + 1.07597i	19.7896 + 1.12859i	
	10	1	9.31753 + 0.814768i	12.3012 + 1.41244i	19.1551 + 0.82638i	
		5	9.77316 + 0.876151i	14.0075 + 1.28874i	20.1141 + 0.888704i	
		10	9.92933 + 0.920608i	15.3104 + 1.14153i	21.8502 + 0.991453i	

Table 2 presents the variation of dimensionless frequencies for a viscoelastic nanotube depending on the scale parameter and bond forces. As a result of the calculations, the frequency values have been obtained as complex numbers; the real part of these numbers represents the frequency of the vibration, while the imaginary part represents the damping in the system. However, the values presented in table format are limited in comprehensively evaluating the effects of the parameters on the dynamic response of the structure. Therefore, in order to examine more clearly and comparatively how the viscoelastic properties, bond forces, and size effects are reflected in the dynamic behavior of the system, the results are presented and discussed with figures.

Figure 3 displays the relationship between frequency and damping obtained by considering viscoelastic effects. A clear mathematical relationship is observed between the frequency and damping values for single-walled nanotubes. As frequently emphasized in the literature, this relationship is expressed as the sum of the squares of frequency and damping being equal to the square of the undamped frequency. In other words, it is possible to mention a circular relationship between frequency and damping. In contrast, it is difficult to mention the direct existence of a similar relationship in a triple-walled nanotube; however, it is observed that the system gradually approaches this circular relationship with the increase in bond forces.

Figure 4 illustrates a three-dimensional graph indicating how dimensionless frequencies change with variation in bond forces. The frequency value obtained in this way is for the first root in the first mode. Here, it is considered that as bond forces increase, the ease with which sections transfer load to each other in other words, the increase in rigidity has been carried out, leading to an increase in frequency. Furthermore, the reason why the increase in c_2 increases the dimensionless frequency more is directly related to the fact that the combination of the second and third walls has a larger cross-sectional area.

Figure 5 indicates the variation in dimensionless frequency depending on the viscous damping parameter for three roots. Real values decrease as the viscous damping parameter increases, while imaginary values increase approximately linearly. Furthermore, when the real values reach zero, the imaginary values exhibit a nonlinear increase. Another noteworthy point here is that the root with the smallest frequency value in the undamped vibration ceases to be the dominant vibration mode as the viscous damping parameter increases. This can be attributed to the viscous damping parameter having a greater effect on higher frequencies.

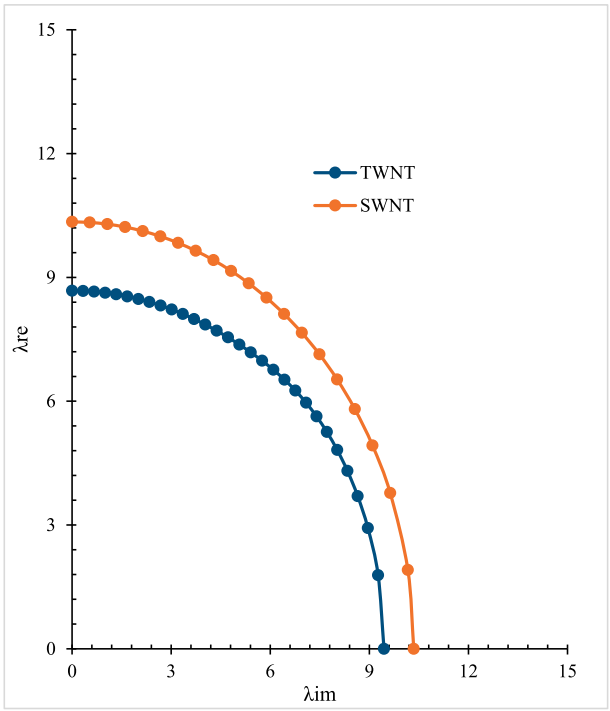


Fig. 3 Relationship between the real and imaginary values of the frequencies of viscoelastic triple-walled and single-walled nanotubes

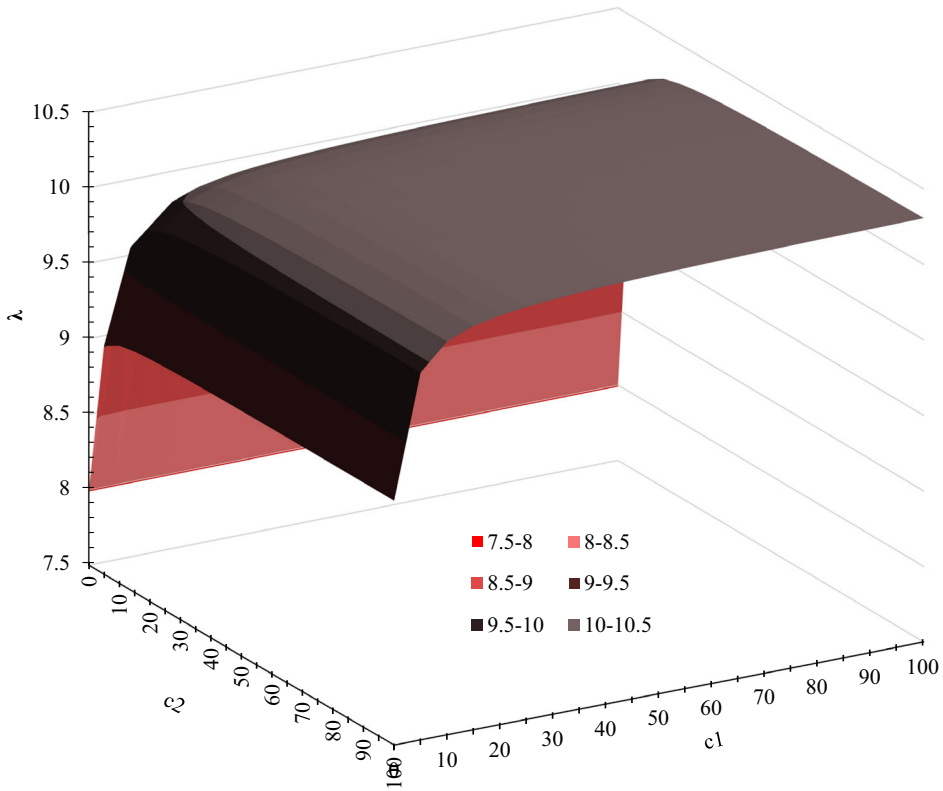


Fig. 4 Change in dimensionless frequencies depending on the change in bond forces

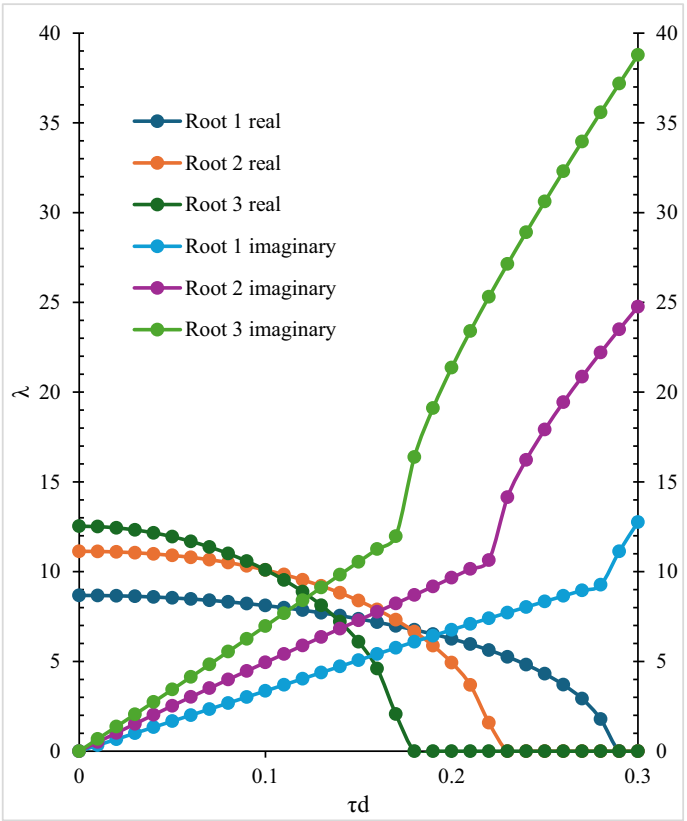


Fig. 5 Change in dimensionless frequencies for three roots depending on the viscous damping parameter in the first mode

Figure 6 demonstrates the variation in dimensionless frequencies depending on the viscous damping parameter for different bond force values. As bond forces increase, the structure exhibits more rigid structural behavior. Therefore, it is not incorrect to state that the effect of damping is greater for larger bond force values, as damping has a greater effect on more rigid structures.

A graph has been constructed illustrating how dimensionless frequencies change depending on the viscous damping parameter for different scale parameters in Fig. 7. Upon examining the graph, it can be stated that the real values of the dimensionless frequencies decline as the viscous damping parameter rises, while the imaginary values increase in an approximately linear trend until the real values reach zero, after which this linearity breaks down and an increasingly rising trend is observed. Furthermore, it would not be wrong to claim that an increment in the scale parameter has an enhancing effect on the beam's stiffness. Consequently, it is evident that the increasing stiffness effects will also enhance the damping effect. As a result, it can be stated that an increase in the scale parameter enhances the effect of the viscous damping parameter on the dimensionless frequency.

It has already been mentioned that three roots will be obtained when investigating the frequency of a triple-walled nanotube. It is predicted that the smallest of these roots corresponds to the frequency that enables the walls to vibrate in harmony with each other. Figure 8 indicates the variation of these three roots depending on the scale parameter. Furthermore, to include information on how the frequency changes when this cross section is considered as a single-walled nanotube, the variation in dimensionless frequencies depending on the scale parameter in a single-walled nanotube has been presented. This graph reveals that an increase in the scale parameter causes a greater frequency increase in the dimensionless frequency of the single-walled nanotube compared to the other roots. This may be due to the lower rigidity of beams with weak bonds. In other words, the stiffness-enhancing effects of the scale parameter can be associated with a more limited increase in stiffness for triple-walled nanotubes.

Figure 9 displays the variation in damped and undamped dimensionless frequencies depending on the variation in the scale parameter. An increase in the scale parameter causes an increase in frequency due to its stiffness-enhancing effect on undamped vibration. This is supported by numerous studies. However, as can be

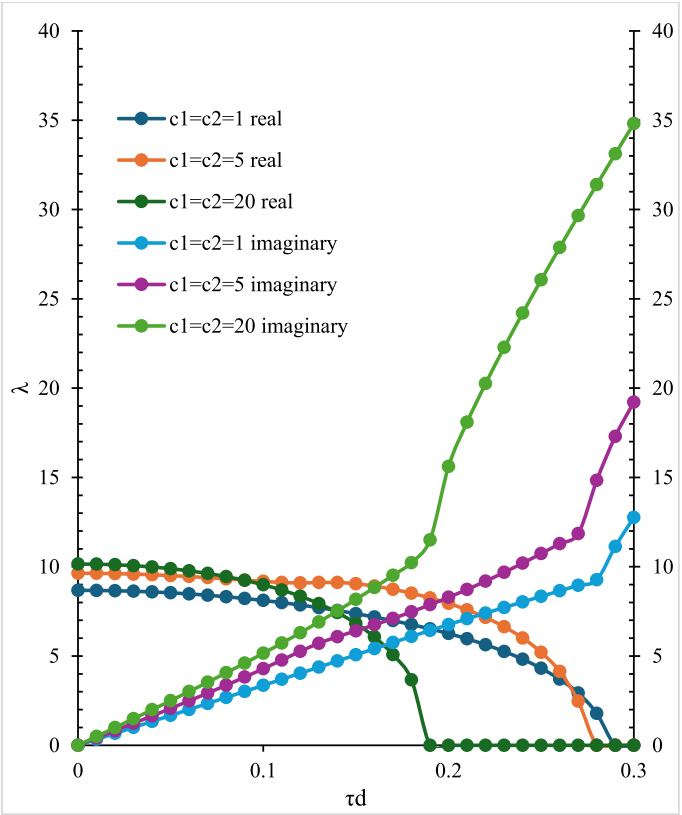


Fig. 6 Change in dimensionless frequencies depending on the change in viscous damping parameter at different bond strengths

observed in the figure, as the viscous damping parameter increases, this enhancing effect is seen to transform into a reducing effect at a certain point. This point can be said to start from the point where the real value of the dimensionless frequency for damped vibration is smaller than the imaginary value. The fundamental reason for this variation may be related to the fact that the viscous damping parameter does not have an equal effect for each value of the scale parameter.

Figure 10 illustrates the variation in the dimensionless frequencies of triple-walled and single-walled nanotubes depending on modal effects. Here, the mode increase for TWNT represents the smallest root obtained in each mode. As the number of modes increases, the dimensionless frequency also increases. This is related to the transformation of single-bending vibrations into multi-bending vibration modes with the increase in modes. Stiffness is considered the fundamental parameter for the formation of these bends. Therefore, it is thought that as the mode number increases, the frequency values of single-walled and triple-walled nanotubes diverge from each other.

This study examines the free vibration behavior of triple-walled viscoelastic nanotubes, revealing the effects of inter-wall bond forces and viscoelastic damping properties on the dynamic response. However, the results are based on a theoretical model developed under certain assumptions; therefore, the validity of the model is limited in terms of the accuracy of the assumptions used and the need for experimental data to support them. Furthermore, since only linear viscoelastic behavior has been considered, possible nonlinear effects are beyond the scope of this study. Nevertheless, the findings represent an important step in understanding how the vibration characteristics of multi-walled nanotubes differ from those of single-walled structures. In particular, the pronounced effects of bond forces and nanoscale effects on dynamic parameters can be considered an important design criterion to be taken into account in the design of future nanomechanical systems. Therefore, this study can serve as a fundamental reference for both theoretical and applied aspects of ongoing research aimed at understanding the vibration and damping behavior of nanostructures.

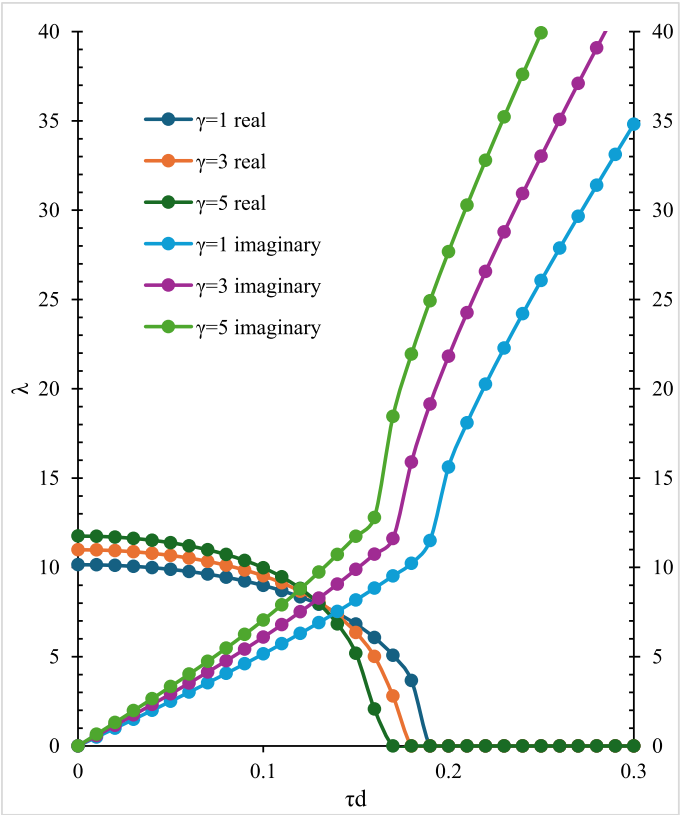


Fig. 7 Change in dimensionless frequencies depending on the viscous damping parameter for different scale parameters

5 Conclusions

This study investigates the free vibration of triple-walled viscoelastic nanotubes. The research has revealed that the bond forces between the walls of triple-walled nanotubes have significant effects on the dynamic behavior of the structure. It has been found that as the bond forces increase, the frequency of the structure converges to the frequency value obtained for a single-walled nanotube. It has also been observed that the increase in these bond forces affects the frequency of the system in proportion to the rigidity of the bonded walls. Furthermore, it has been observed that the nanoscale effects increase with the increase in bond forces.

Stress-based size effects have stiffness-enhancing effects. These effects are proportional to the size of the area they affect; therefore, the greater the bond forces, the greater the effect of the scale parameter.

With modal growth, the dimensionless frequencies of single-walled nanotubes and triple-walled nanotubes begin to diverge.

Furthermore, this study also investigates the damping effects on the system by including viscoelastic properties. Although damping is a highly complex phenomenon, some conclusions can be drawn. In the viscoelastic model used, there is a mathematical relationship between the imaginary and real values of the frequencies obtained for single-walled nanotubes, while no such relationship exists for triple-walled nanotubes. The effect of damping increases as the scale parameter increases. However, it has been observed that from the point where the viscous damping parameter is smaller than the imaginary values of the real frequencies, the known effects of the scale parameter vary completely in the opposite direction. It is thought that this may be due to the viscous damping parameter not having the same effect for each scale parameter value. An increase in the viscous damping parameter reduces the real values of the frequency while increasing the imaginary values approximately in a linear fashion. It can also be said that the slope of these lines is effective in determining the effect of damping.

The free vibration characteristics of the three-layered viscoelastic nanotubes examined in our study have direct application potential in areas such as vibration control of nanocomposite materials, nanosensor design, and nanoscale energy harvesting systems. Furthermore, the developed stress-driven model can more accurately

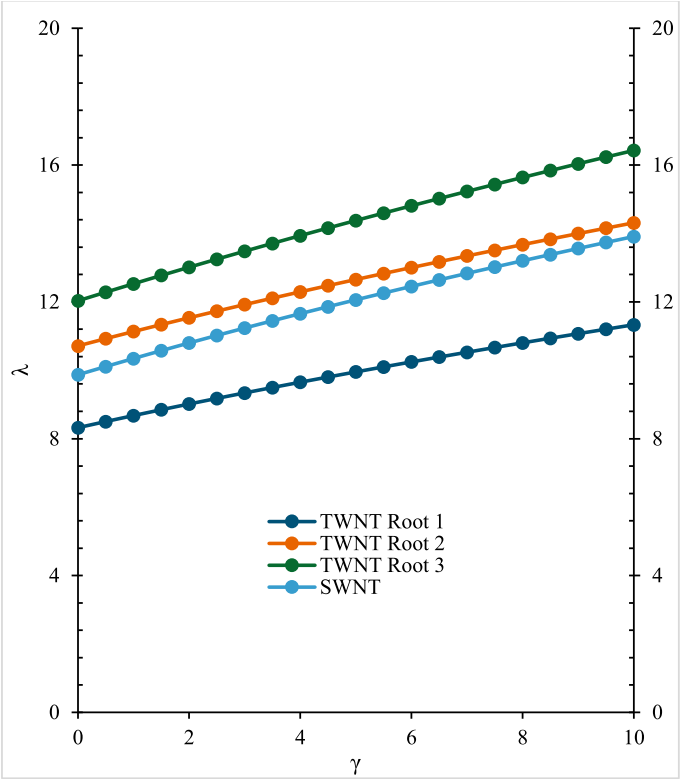


Fig. 8 Dimensionless frequency roots of a triple-walled nanotube and the dimensionless frequency of a single-walled nanotube as a function of the scale parameter

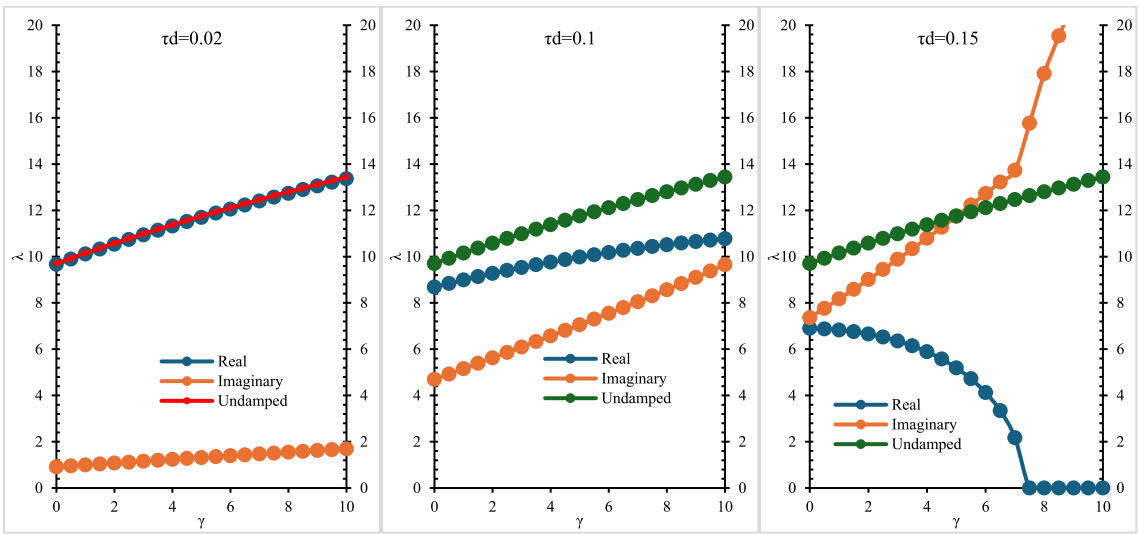


Fig. 9 Change in the dimensionless frequencies of triple-walled nanotubes with different viscous damping parameter values according to the scale parameter

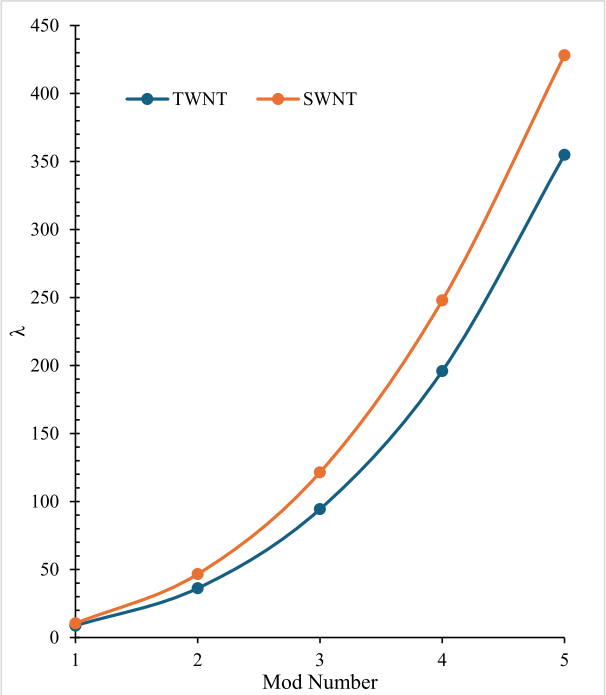


Fig. 10 Change in the frequencies of triple-walled and single-walled nanotubes according to the number of modes

predict the mechanical behavior of multilayered systems at the nanoscale, making it applicable in various disciplines such as materials engineering, nanoelectronics, and biomechanical system design.

Acknowledgements This study was supported by the Scientific Research Projects Coordination Unit of Bursa Uludağ University under project number Performance-Based Support Projec-2025-2339. The author gratefully acknowledges the financial support provided.

Author contributions All authors contributed equally to the manuscript.

Funding Open access funding provided by the Scientific and Technological Research Council of Türkiye (TÜBİTAK). No funding was provided for the conduct of this study.

Data availability Datasets generated during the current study are available from the corresponding author on reasonable request.

Declarations

Conflict of interest The authors declare no competing interests.

Open Access This article is licensed under a Creative Commons Attribution 4.0 International License, which permits use, sharing, adaptation, distribution and reproduction in any medium or format, as long as you give appropriate credit to the original author(s) and the source, provide a link to the Creative Commons licence, and indicate if changes were made. The images or other third party material in this article are included in the article's Creative Commons licence, unless indicated otherwise in a credit line to the material. If material is not included in the article's Creative Commons licence and your intended use is not permitted by statutory regulation or exceeds the permitted use, you will need to obtain permission directly from the copyright holder. To view a copy of this licence, visit http://creativecommons.org/licenses/by/4.0/.

References

1. Wang, C.M., Tan, V.B.C., Zhang, Y.Y.: Timoshenko beam model for vibration analysis of multi-walled carbon nanotubes. J. Sound Vib. **294**, 1060–1072 (2006). https://doi.org/10.1016/j.jsv.2006.01.005

2. Natsuki, T., Ni, Q.-Q., Endo, M.: Analysis of the vibration characteristics of double-walled carbon nanotubes. Carbon **46**, 1570–1573 (2008). https://doi.org/10.1016/j.carbon.2008.06.058
3. Natsuki, T., Lei, X.-W., Ni, Q.-Q., Endo, M.: Free vibration characteristics of double-walled carbon nanotubes embedded in an elastic medium. Phys. Lett. A **374**, 2670–2674 (2010). https://doi.org/10.1016/j.physleta.2010.04.040
4. Yan, Y., He, X.Q., Zhang, L.X., Wang, C.M.: Dynamic behavior of triple-walled carbon nanotubes conveying fluid. J. Sound Vib. **319**, 1003–1018 (2009). https://doi.org/10.1016/j.jsv.2008.07.001
5. Zhang, D.P., Lei, Y., Shen, Z.B.: Free transverse vibration of double-walled carbon nanotubes embedded in viscoelastic medium. Acta Mech. **227**, 3657–3670 (2016). https://doi.org/10.1007/s00707-016-1686-2
6. Pentaras, D., Elishakoff, I.: Free vibration of triple-walled carbon nanotubes. Acta Mech. **221**, 239–249 (2011). https://doi.org/10.1007/s00707-011-0496-9
7. Artan, R., Tepe, A.: Nonlocal effects in curved single-walled carbon nanotubes. Mech. Adv. Mater. Struct. (2011). https://doi.org/10.1080/15376494.2010.516885
8. Tepe, A.: Nonlocal effects on curved double-walled carbon nanotubes based on nonlocal theory. Arch. Appl. Mech. **95**, 57 (2025). https://doi.org/10.1007/s00419-025-02762-2
9. Aydogdu, M.: A nonlocal rod model for axial vibration of double-walled carbon nanotubes including axial van der Waals force effects. J. Vib. Control (2014). https://doi.org/10.1177/1077546313518954
10. Ehyaei, J., Daman, M.: Free vibration analysis of double walled carbon nanotubes embedded in an elastic medium with initial imperfection. Adv. Nano. Res.**1**(5) 179–192 (2017)
11. Murmu, T., McCarthy, M.A., Adhikari, S.: Vibration response of double-walled carbon nanotubes subjected to an externally applied longitudinal magnetic field: a nonlocal elasticity approach. J. Sound Vib. **331**, 5069–5086 (2012). https://doi.org/10.1016/j.jsv.2012.06.005
12. Shen, Z.-B., Tang, G.-J., Zhang, L., Li, X.-F.: Vibration of double-walled carbon nanotube based nanomechanical sensor with initial axial stress. Comput. Mater. Sci. **58**, 51–58 (2012). https://doi.org/10.1016/j.commatsci.2012.02.011
13. Dihaj, A., Zidour, M., Meradjah, M., Rakrak, K., Heireche, H., Chemi, A.: Free vibration analysis of chiral double-walled carbon nanotube embedded in an elastic medium using non-local elasticity theory and Euler Bernoulli beam model | DBpia. (2018)
14. Rakrak, K., Zidour, M., Heireche, H., Bousahla, A.A., Chemi, A.: Free vibration analysis of chiral double-walled carbon nanotube using non-local elasticity theory. Adv. Nano. Res.**1**(4), 31–44 (2016)
15. Kiani, K.: Characterization of free vibration of elastically supported double-walled carbon nanotubes subjected to a longitudinally varying magnetic field. Acta Mech. **224**, 3139–3151 (2013). https://doi.org/10.1007/s00707-013-0937-8
16. Kiani, K.: Longitudinally varying magnetic field influenced transverse vibration of embedded double-walled carbon nanotubes. Int. J. Mech. Sci. **87**, 179–199 (2014). https://doi.org/10.1016/j.ijmecsci.2014.04.018
17. Lee, H.-L., Chang, W.-J.: Vibration analysis of fluid-conveying double-walled carbon nanotubes based on nonlocal elastic theory. J. Phys. Condens. Matter **21**, 115302 (2009). https://doi.org/10.1088/0953-8984/21/11/115302
18. Aydogdu, M., Arda, M.: Torsional vibration analysis of double walled carbon nanotubes using nonlocal elasticity. Int. J. Mech. Mater. Des. **12**, 71–84 (2016). https://doi.org/10.1007/s10999-014-9292-8
19. Mohamadi, B., Eftekhari, S.A., Toghraie, D.: Numerical investigation of nonlinear vibration analysis for triple-walled carbon nanotubes conveying viscous fluid. Int. J. Numer. Methods Heat Fluid Flow **30**, 1689–1723 (2019). https://doi.org/10.1108/HFF-10-2018-0600
20. Channakote, M.M., Marudappa, S., Bég, O.A., Narayana, M., Siddabasappa, C.: Electro-osmotic peristaltic streaming of a fractional second-grade viscoelastic nanofluid with single and multi-walled carbon nanotubes in a ciliated tube. Results Eng. **26**, 104739 (2025). https://doi.org/10.1016/j.rineng.2025.104739
21. Zeighampour, H., Tadi Beni, Y.: Size-dependent vibration of fluid-conveying double-walled carbon nanotubes using couple stress shell theory. Phys. E Low-Dimens. Syst. Nanostruct. **61**, 28–39 (2014). https://doi.org/10.1016/j.physe.2014.03.011
22. Yıldız, T., Esen, I.: On the effect of the Casimir, van der Waals and electrostatic forces on the thermomechanical buckling of sandwich smart piezo magnetic nanosensor/switch plates. Microsyst. Technol. **31**, 1525–1545 (2025). https://doi.org/10.1007/s00542-024-05813-w
23. Özmen, R., Esen, I.: The Casimir, Van der Waals, and electrostatic forces' effects on the response of magneto-electro-elastic nanosensor/switch beams under thermal environment. Mech. Based Des. Struct. Mach. **52**, 8294–8320 (2024). https://doi.org/10.1080/15397734.2024.2318615
24. Romano, G., Barretta, R.: Nonlocal elasticity in nanobeams: the stress-driven integral model. Int. J. Eng. Sci. **115**, 14–27 (2017). https://doi.org/10.1016/j.ijengsci.2017.03.002
25. Romano, G., Barretta, R.: Stress-driven versus strain-driven nonlocal integral model for elastic nano-beams. Compos. Part B Eng. **114**, 184–188 (2017). https://doi.org/10.1016/j.compositesb.2017.01.008
26. Luciano, R., Darban, H., Bartolomeo, C., Fabbrocino, F., Scorza, D.: Free flexural vibrations of nanobeams with non-classical boundary conditions using stress-driven nonlocal model. Mech. Res. Commun. **107**, 103536 (2020). https://doi.org/10.1016/j.mechrescom.2020.103536
27. Faraji Oskouie, M., Ansari, R., Rouhi, H.: Stress-driven nonlocal and strain gradient formulations of Timoshenko nanobeams. Eur. Phys. J. Plus **133**, 336 (2018). https://doi.org/10.1140/epjp/i2018-12183-x
28. Akpınar, M., Uzun, B., Kadıoğlu, H.G., Yaylı, M.Ö.: Dynamic analysis of restrained short-fiber-reinforced and functionally graded nanobeams via stress-driven model. ZAMM J. Appl. Math. Mech. (2025). https://doi.org/10.1002/zamm.70133
29. Altekin, M., Karatas, E.E., Yükseler, R.F.: Stress-driven nonlocal theory on nonlinear static analysis of annular nanoplates. Mech. Based Des. Struct. Mach. **53**, 6283–6328 (2025). https://doi.org/10.1080/15397734.2025.2480706
30. Tekin Atacan, A., Yükseler, R.F.: Size-dependent snap buckling behavior of functionally graded sinusoidal shallow nanoarches supported by elastic horizontal springs using the stress-driven nonlocal approach. Mech. Res. Commun. **148**, 104487 (2025). https://doi.org/10.1016/j.mechrescom.2025.104487
31. Tadi Beni, Y.: Size dependent torsional electro-mechanical analysis of flexoelectric micro/nanotubes. Eur. J. Mech. A. Solids **95**, 104648 (2022). https://doi.org/10.1016/j.euromechsol.2022.104648

32. Tadi Beni, Y.: Size dependent coupled electromechanical torsional analysis of porous FG flexoelectric micro/nanotubes. Mech. Syst. Signal Process. **178**, 109281 (2022). https://doi.org/10.1016/j.ymssp.2022.109281
33. Kadioglu, H.G., Uzun, B., Yayli, M.O.: Dynamic torsional response of viscoelastic porous nanorods with viscoelastic boundary constraints. Arab. J. Sci. Eng. (2025). https://doi.org/10.1007/s13369-025-10208-8
34. Kadioglu, H.G., Uzun, B., Yayli, M.O.: Size-dependent vibration analysis of a FG viscoelastic nanotube attached with the time-dependent boundary conditions using NLSGT. ZAMM J. Appl. Math. Mech. **105**, e202400934 (2025). https://doi.org/10.1002/zamm.202400934
35. Kadıoğlu, H.G., Yaylı, M.Ö.: Analysis of torsional vibration in viscoelastic functionally graded nanotubes with viscoelastic constraints using doublet mechanics theory. Int. J. Mech. Mater. Des. (2025). https://doi.org/10.1007/s10999-025-09802-3
36. Barretta, R., Faghidian, S.A., Marotti De Sciarra, F., Penna, R., Pinnola, F.P.: On torsion of nonlocal Lam strain gradient FG elastic beams. Compos. Struct. **233**, 111550 (2020). https://doi.org/10.1016/j.compstruct.2019.111550
37. Esen, I., Daikh, A.A., Eltaher, M.A.: Dynamic response of nonlocal strain gradient FG nanobeam reinforced by carbon nanotubes under moving point load. Eur. Phys. J. Plus **136**, 458 (2021). https://doi.org/10.1140/epjp/s13360-021-01419-7
38. Abdelrahman, A.A., Esen, I., Özarpa, C., Eltaher, M.A.: Dynamics of perforated nanobeams subject to moving mass using the nonlocal strain gradient theory. Appl. Math. Model. **96**, 215–235 (2021). https://doi.org/10.1016/j.apm.2021.03.008
39. Mirfatah, S.M., Salehipour, H., Civalek, Ö.: On the nonlinear forced vibration of nanoshells via nonlocal strain gradient theory. Int. J. Eng. Sci. **211**, 104257 (2025). https://doi.org/10.1016/j.ijengsci.2025.104257
40. Civalek, Ö., Uzun, B., Yaylı, M.Ö.: Longitudinal vibration analysis of FG nanorod restrained with axial springs using doublet mechanics. Waves in Random and Complex Media. https://doi.org/10.1080/17455030.2021.2000675 (2024)
41. Eltaher, M.A., Abdelrahman, A.A., Esen, I.: Dynamic analysis of nanoscale Timoshenko CNTs based on doublet mechanics under moving load. Eur. Phys. J. Plus **136**, 705 (2021). https://doi.org/10.1140/epjp/s13360-021-01682-8
42. Civalek, Ö., Akgöz, B.: Bending analysis of CNT-reinforced composite strain gradient microbeams. Mech. Res. Commun. **148**, 104502 (2025). https://doi.org/10.1016/j.mechrescom.2025.104502
43. Yıldırım, A., Akgöz, B.: Buckling behavior of nickel microbeams based on reformulated strain gradient theory. Appl. Phys. A **130**, 832 (2024). https://doi.org/10.1007/s00339-024-08013-5
44. Challamel, N., El-Borgi, S., Trabelssi, M., Reddy, J.N.: Free vibration response of micromorphic Timoshenko beams. J. Sound Vib. **591**, 118602 (2024). https://doi.org/10.1016/j.jsv.2024.118602
45. El-Borgi, S., Rajendran, P., Friswell, M.I., Trabelssi, M., Reddy, J.N.: Torsional vibration of size-dependent viscoelastic rods using nonlocal strain and velocity gradient theory. Compos. Struct. **186**, 274–292 (2018). https://doi.org/10.1016/j.compstruct.2017.12.002
46. Dehkordi, H.R.B., Beni, Y.T.: Size-dependent coupled bending-torsional analysis of piezoelectric micro beams. Mech. Based Des. Struct. Mach. **52**, 6484–6506 (2024)
47. Hosseini, S.M.H., Beni, Y.T.: On the vibration of size-dependent rotating flexoelectric microbeams. Appl. Phys. A **130**, 58 (2024). https://doi.org/10.1007/s00339-023-07207-7
48. Uzun, B.: Magnetic field and non-local effects on axial vibration of embedded nanorods reinforced with short fibers. Acta Mech. **236**, 4889–4920 (2025). https://doi.org/10.1007/s00707-025-04417-3
49. Özmen, R., Esen, I.: Dynamic response of embedded Timoshenko CNTs exposed to magnetic and thermal fields subjected to moving load based on doublet mechanics. J. Braz. Soc. Mech. Sci. Eng. **45**, 590 (2023). https://doi.org/10.1007/s40430-023-04506-1
50. Esen, I.: Dynamics of size-dependant Timoshenko micro beams subjected to moving loads. Int. J. Mech. Sci. **175**, 105501 (2020). https://doi.org/10.1016/j.ijmecsci.2020.105501
51. Dehkordi, H.R.B., Beni, Y.T.: Size-dependent coupled bending-torsional vibration of functionally graded carbon nanotube reinforced composite Timoshenko microbeams. Arch.Civ.Mech.Eng **23**, 186 (2023). https://doi.org/10.1007/s43452-023-00725-4
52. Kadıoğlu, H.G., Uzun, B., Civalek, Ö., Yaylı, M.Ö.: Dynamic behavior of micromorphic viscoelastic Euler–Bernoulli beams under viscoelastic boundary constraints. Acta Mech. **236**, 4475–4490 (2025). https://doi.org/10.1007/s00707-025-04364-z
53. Kadioglu, H.G., Yayli, M.O.: Modified Jeffreys viscoelastic model for axial vibration of nanorods with realistic boundary conditions. Eur. Phys. J. Plus. **140**, 672 (2025). https://doi.org/10.1140/epjp/s13360-025-06596-3

Publisher's Note Springer Nature remains neutral with regard to jurisdictional claims in published maps and institutional affiliations.